

See discussions, stats, and author profiles for this publication at: <https://www.researchgate.net/publication/265641608>

# Longitudinal and lateral control for autonomous ground vehicles

Conference Paper · June 2014

DOI: 10.1109/IVS.2014.6856431

CITATIONS

13

READS

519

4 authors:



**Carlos M. Massera**

University of São Paulo

18 PUBLICATIONS 50 CITATIONS

[SEE PROFILE](#)



**Denis Wolf**

University of São Paulo

142 PUBLICATIONS 1,447 CITATIONS

[SEE PROFILE](#)



**Valdir Grassi Jr**

University of São Paulo

34 PUBLICATIONS 337 CITATIONS

[SEE PROFILE](#)



**Fernando Osorio**

University of São Paulo

184 PUBLICATIONS 1,041 CITATIONS

[SEE PROFILE](#)

Some of the authors of this publication are also working on these related projects:



Safety guarantees for Cooperative Adaptive Cruise Control (CACC) based on Robust Model Predictive Control [View project](#)



Perception methods for object detection and tracking in urban scenarios [View project](#)

# Longitudinal and Lateral Control for Autonomous Ground Vehicles

Carlos Massera Filho<sup>1</sup>, Denis F. Wolf<sup>1</sup>, Valdir Grassi Jr<sup>2</sup>, Fernando S. Osório<sup>1</sup>

**Abstract**—Robust and stable control is a requirement for navigation of self-driving cars. Some approaches in the literature depend on a high number of parameters that are often difficult to estimate. A poor selection of these parameters often reduces considerably the efficiency of the control algorithms. In this paper we propose a simplified control system for autonomous vehicles that depends on a reduced number of parameters that can be easily set. This control system is composed of longitudinal and lateral controllers. The longitudinal controller is responsible for regulating the vehicle's cruise velocity while the lateral controller steers the vehicle's wheels for path tracking. Simulated and experimental tests have been carried out with the CaRINA II platform in the university campus with positive results.

## I. INTRODUCTION

Autonomous navigation for intelligent vehicles usually requires a control system for path following. This control system is composed of longitudinal and lateral controllers. The longitudinal controller is responsible for regulating the vehicle's cruise velocity while the lateral controller steers the vehicle's wheels for path tracking.

A review of commonly used steering control laws, with analysis and comparison of results obtained through simulation were presented in [1]. This review includes some steering control approaches used by DARPA Grand Challenge and Urban Challenge vehicles, such as, Sandstorm, Stanley, and Boss. Sandstorm, the vehicle placed in second in DARPA Grand Challenge, uses a modified version of the pure-pursuit path tracking controller [2], [3], in which, they introduced an integral term to the controller in order to remove the steady-state lateral offset error caused by the shifting steering angle sensor of the vehicle [4]. Stanley and Junior, the vehicles placed in first in DARPA Grand Challenge and second in DARPA Urban Challenge, used a steering control law based on vehicle's kinematic model [5]. Boss, the vehicle that won DARPA Urban Challenge, used a model predicted control strategy [6]. Another Urban Challenge participant, OSU-ACT car, used an approach called circular look-ahead (CLA) [7] proposed to improve curve following accuracy. This approach takes into account the curvature of the path to be followed and the Dubin's car kinematic model to represent the vehicle.

In this paper we present the control system developed for our autonomous vehicle named CaRINA II (Figure 1). As the autonomous vehicle's control systems previously described,



Fig. 1. Fiat Palio Adventure known as CaRINA II, used in experiments

we have also decoupled the longitudinal and lateral control. However, our approach have some particularities which distinguishes from the other. Some approaches for path tracking in the literature depend on a high number of parameters that are often difficult to estimate. A poor selection of these parameters often reduces considerably the efficiency of the control algorithms. Here we propose a simplified control system for autonomous vehicles that depends on a reduced number of parameters that can be easily set.

We have derived a longitudinal dynamic model, in which we consider the vehicle moving on an inclined road, in order to establish the relationship between desired acceleration and throttle or brake pedal position. The control law developed considers the road curvature to limit the maximum safe cruise velocity based on the maximum lateral acceleration of the vehicle. Then the current vehicle acceleration is computed so that the vehicle's velocity converges exponentially to the desired safe velocity.

For path tracking, a lateral controller is used together with the longitudinal controller. The non-linear lateral controller proposed here uses a cubic Belzier curve to find a short trajectory, starting from the current vehicle's pose, which converges to the planned trajectory to be tracked. The vehicle follows this short trajectory setting the wheel's steering angle to a value computed using the current cruise velocity and the yaw derivative of the cubic Belzier curve. From time to time the Belzier curve is updated providing a new reference for the controller.

This paper is organized as follows: Section 2 describes the longitudinal and lateral vehicle modelling. Section 3 describes the proposed controllers. Section 4 presents the

<sup>1</sup>Institute of Mathematics and Computer Science, University of São Paulo, Avenida Trabalhador São-carlense, 400, São Carlos, Brazil [massera,denis,fosorio@icmc.usp.br](mailto:massera,denis,fosorio@icmc.usp.br)

<sup>2</sup>São Carlos School of Engineering, University of São Paulo, Avenida Trabalhador São-carlense, 400, São Carlos, Brazil [vgrassi@usp.br](mailto:vgrassi@usp.br)

experimental results. In Section 5 we discuss the results, and in Section 6 we draw some conclusions and comment about future work.

## II. VEHICLE MODELING

This section describes a longitudinal and a lateral model for vehicle dynamics. The first is a time-invariant simplification of acceleration, braking and resistance forces. The lateral model is based on the planar bicycle model, a simplification of Ackermann's model where the vehicle consists of two wheels on top of its center line.

### A. Longitudinal Model

A longitudinal model for a vehicle can be expressed by Newton's second law [8], where its acceleration can be defined in terms of air drag ( $F_{air}$ ), internal resistances ( $F_{int}$ ), rolling resistance ( $F_{rr}$ ), gravitational forces ( $F_{gr}$ ), engine force ( $F_{ice}$ ), braking forces ( $F_{brake}$ ) and vehicle mass ( $m_v$ ) as:

$$m_v \dot{v} = F_{ice} + F_{brake} + F_{air} + F_{rr} + F_{gr} + F_{int} \quad (1)$$

The engine force is  $F_{ice} = \frac{f_g e_{dt}}{r_w} \tau_{ice}(\alpha, \omega)$  where  $f_g$  is the gear ratio,  $e_{dt}$  the drivetrain efficiency,  $r_w$  the wheel radius and  $\tau_{ice}(\alpha, \omega)$  the internal combustion engine (ICE) mapping based on engine angular speed  $\omega$  and throttle pedal position  $\alpha$  given  $\alpha \in [0, 1]$ . The gravity force is  $F_{gr} = m_v g \sin(\theta)$ , where  $\theta$  is the vehicle pitch.

In order to obtain the brake force model, the vehicle was driven multiple times in a road with negligible inclination where at different speeds the brake pedal was pressed at several points and the generated acceleration was measured. From this data the model was obtained from a linear regression of the resultant acceleration generated given the brake pedal position ( $\beta$ ) and the vehicle speed ( $v$ ). Resulting in  $\dot{v}_{brake}(\beta, v) = \frac{F_{brake}}{m_v} = \min(0, 2.27 - 6.12\beta + 0.00535v)$  given  $\beta \in [0, 1]$ .

With the purpose of obtaining a simplified model, air drag, rolling resistances and internal forces were assumed to be negligible and the vehicle never accelerates and brakes simultaneously, therefore either  $F_{ice} = 0$  or  $F_{brake} = 0$ . Based on these assumptions we can define the longitudinal vehicle model as:

$$\dot{v} = \begin{cases} \frac{f_g e_{dt}}{r_w m_v} \tau_{ice}(\alpha, \omega) - g \sin(\theta) & \alpha \geq 0, \beta = 0 \\ \dot{v}_{brake}(\beta, v) - g \sin(\theta) & \beta \geq 0, \alpha = 0 \end{cases} \quad (2)$$

Based on Equation 2 and defining  $\tau_{ice}^{-1}(\tau_d, \omega)$  as the inverse ICE map and  $\dot{v}_{brake}^{-1}(\dot{v}_d, v)$  as the inverse brake model, the inverse longitudinal vehicle model is given by Equations 3 and reffbeta where  $\tau_d = r_{dt} \dot{v}_d$  is the desired output torque,  $\dot{v}_d$  the desired acceleration and  $r_{dt} = \frac{r_w m_v}{f_g e_{dt}}$  the drivetrain ratio between engine torque and vehicle acceleration.

$$\alpha = \begin{cases} \tau_{ice}^{-1}(r_{dt}(\dot{v}_d + g \sin(\theta)), \omega) & \dot{v}_d + g \sin(\theta) > 0 \\ 0 & otherwise \end{cases} \quad (3)$$

$$\beta = \begin{cases} \dot{v}_{brake}^{-1}(\dot{v}_d + g \sin(\theta), v) & \dot{v}_d + g \sin(\theta) < 0 \\ 0 & otherwise \end{cases} \quad (4)$$

From the equations 3 and 4 above it is possible to determine throttle and brake pedal positions from a desired acceleration and a vehicle pitch.

### B. Lateral Model

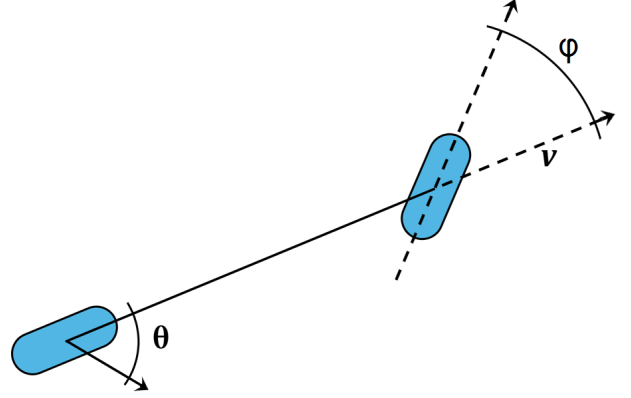


Fig. 2. Bicycle Model

Previous works [8] [9] demonstrated that a bicycle model, shown in Figure 2, can be used as a good approximation for a low speed vehicle lateral model. The two left and right front wheels are represented as one single front wheel and similarly the left and right rear wheels are also represented as one wheel. It is assumed that the rear virtual wheel do not steer and  $\varphi$  is defined as the front virtual wheel steering angle.

This model considers motion in x axis, y axis and yaw  $\theta$  given  $\varphi$  as a control input. Assuming a negligible tire slip, the model translates into the motion constrains in Equation 5 where  $(v_x^f, v_y^f)$  and  $(v_x^b, v_y^b)$  are pairs of x-y axis velocities for the front and back wheels, respectively [10].

$$\begin{aligned} v_x^f \sin(\theta + \varphi) - v_y^f \cos(\theta + \varphi) &= 0 \\ v_x^b \sin(\theta) - v_y^b \cos(\theta) &= 0 \end{aligned} \quad (5)$$

The solution for the constrains in Equation 5 corresponds to the kinematic model of a car-like vehicle shown in Equation 6 where  $v(t)$  is the vehicle's speed,  $\theta$  its yaw angle and  $l$  its length.

$$\begin{bmatrix} \dot{x}(t) \\ \dot{y}(t) \\ \dot{\theta}(t) \end{bmatrix} = \begin{bmatrix} v(t) \cos(\theta(t)) \\ v(t) \sin(\theta(t)) \\ \frac{v(t)}{l} \tan(\varphi(t)) \end{bmatrix} \quad (6)$$

## III. CONTROL LAWS

This section describes the longitudinal and lateral control laws and analyzes its stability and convergence. The longitudinal is directly derived from the definition of exponential convergence and the lateral defines a correction trajectory between the vehicle position and the path to be tracked using Bézier curves and follows the defined correction path using an open-loop controller.

### A. Longitudinal Control

This section focuses in describing the behavior and analyzing the stability of the longitudinal control law designed for the CARINA project. The proposed controller has the objective of traveling through roads within the speed limits  $v_{road}^{max}$  and avoiding excessive lateral acceleration on corners  $v_{corner}^{max} = \sqrt{\frac{a_{lateral}^{max}}{\kappa(t)}}$  where  $\kappa(t)$  is the path curvature. Following this principles it is possible to define its goal speed as:

$$v_o = \min \left( v_{road}^{max}, \sqrt{\frac{a_{lateral}^{max}}{\kappa(t)}} \right) \quad (7)$$

Assuming a locally differentiable  $\kappa(t)$  and since  $v_o(t)$  is Lipschitz continuous with a dense and open differentiability domain  $D$  it is possible to define a control law that satisfies a expo constraints presented in Equation 8 if the vehicle jerk is assumed unbounded.

$$v(t) = v_o(t) + (v(0) - v_o(0))e^{-\lambda t} \quad (8)$$

Given  $\lambda > 0$  and differentiating Equation 8 results in a relationship between  $\dot{v}_o(t)$  and the desired acceleration, given in Equation 9.

$$a(t) = \dot{v}_o(t) - \lambda(v(0) - v_o(0))e^{-\lambda t} \quad (9)$$

Substituting Equation 8 in Equation 9 and differentiating 7 results in an asymptotically and exponentially converget control law presented below:

$$a(t) = a_o(t) + \lambda(v_o(t) - v(t)) \quad (10)$$

where:

$$a_o(t) = \begin{cases} -\frac{1}{2\kappa(t)}v_o(t)\dot{\kappa}(t) & v_{corner}^{max} < v_{road}^{max} \\ 0 & otherwise \end{cases} \quad (11)$$

### B. Lateral Control

The proposed nonlinear controller provides tracking of the desired vehicle path as well as the possibility to determine the trajectory used to approach the path. This section details the theory, convergence and stability of the control law.

Given a parametric differentiable path  $\rho^{track}(t)$  it is possible to determine  $t_0$  such that  $\rho^{track}(t_0)$  is the closest point in the path to the vehicles position  $p_0$  and  $t_h$  such that the arclength of  $\rho^{track}(t)$  between  $t_0$  and  $t_h$  equals  $h v(t) + d_0$  where  $h$  is a headway time and  $d_0$  a constant spacing.

Using  $\phi(f(t)) = \text{atan}\left(\frac{\dot{f}_y(t)}{\dot{f}_x(t)}\right)$  as the orientation of a parametric differentiable curve  $f(t)$  it is possible to define a cubic Bézier curve  $\beta^a(t_n), t_n \in [0, 1]$  [11] [12] dependent on a parameter  $\sigma \in [0, +\infty)$  as a correction trajectory to the path with its origin in the vehicle position  $p(t) = [x(t), y(t)]^T$  and direction  $\partial p(\theta(t)) = \|\rho^{track}(t_h) - p(t)\| [\cos(\theta(t)), \sin(\theta(t))]^T$  and its end in  $\rho^{track}(t_h)$  with direction  $\partial \rho^{track}(t_h) = \|\rho^{track}(t_h) - p(t)\| [\cos(\phi(\rho^{track}(t_h))), \sin(\phi(\rho^{track}(t_h)))]^T$  as shown in Equation 12 and Figure 3.

$$\beta^a(t_n) = (1 - t_n)^3 p(t) + (1 - t_n)^2 t_n (p(t) + \sigma \partial p(t)) + (1 - t_n) t_n^2 (\rho^{track}(t_h) - \sigma \partial \rho^{track}(t_h)) + t_n^3 \rho^{track}(t_h) \quad (12)$$

It's worth noticing that both directions  $\partial p(\theta(t))$  and  $\partial \rho^{track}(t_h)$  have its norm equals to the norm between  $p(t)$  and  $\rho^{track}(t_h)$  to avoid skews in the Bézier curve due to high speeds and that the controller performance is heavily influenced by Bézier parameter  $\sigma$  which was optimized in order to minimize arclength while providing asymptotic error norm convergence, resulting in  $\sigma = 0.312$ .

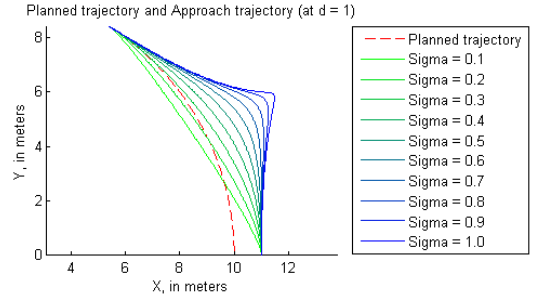


Fig. 3. Correction trajectories generated for  $\sigma \in [0.1, 1]$

Given a cubic Bézier curve  $\beta^a(t_n)$  it is possible to determine the steering for a vehicle at any point  $t_n$  of  $\beta^a(t_n)$  by calculating the path yaw derivative  $\theta^\beta(t_n)$  shown in Equation 13.

$$\dot{\theta}^\beta(t_n) = \frac{\partial \text{atan}\left(\frac{\beta_y^a(t_n)}{\beta_x^a(t_n)}\right)}{\partial t_n} \quad (13)$$

Based on Equation 6, Equation 13 and  $\dot{t}_n = \frac{v(t)}{L^\beta}$  where  $L^\beta$  is the arclength of  $\beta^a(t_n)$  between 0 and 1 its possible to, then, define the necessary steering for following a path  $\varphi^\beta(t)$  as presented in Equation 14 where  $t_0^\beta$  is the closest point from the correction trajectory to the vehicle.

$$\varphi^\beta(t) = \text{atan}\left(\frac{l}{L^\beta} \dot{\theta}^\beta(t_0^\beta)\right) \quad (14)$$

At a given time  $t$  the controller plans a correction trajectory and follows it by calculating  $\varphi^\beta(t)$  until  $t_0^\beta > 0.9$  when a new trajectory is evaluated and followed. Since the steering angle is mechanically limited the control law is defined by Equation 15.

$$\varphi^\beta(t) = \begin{cases} -\varphi^{max} & \varphi^\beta(t) < -\varphi^{max} \\ \varphi^{max} & \varphi^\beta(t) > \varphi^{max} \\ \varphi^\beta(t) & otherwise \end{cases} \quad (15)$$

Behavior analysis of the controller determined that  $\varphi^\beta(t)$  increases monotonically in function of crosstrack error and orientation error, therefore an open-loop controller tracking  $\beta^a(t_n)$  curve is equivalent of a closed-loop controller tracking  $\rho^{track}(t)$ . However, planning a correction trajectory at

each controller cycle causes it to underactuate since for every Bézier curve  $t_n = 0$  and the steering at this point of the curve is not maximum as shown in Figure 4. Choosing a value for  $t_n$  such that  $\varphi^\beta(t)$  is maximized causes the controller to oscillate around the path since it over actuates at all times. For those reasons the vehicle follows the correction curve up to a given point before a new one is evaluated.

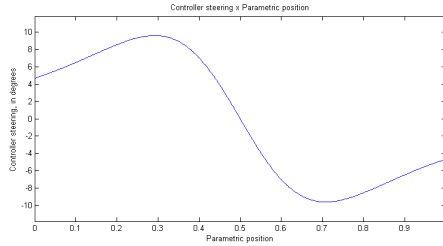


Fig. 4. Steering actuation  $\varphi^\beta(t)$  by parametric position in Bézier curve  $\beta^a(t)$  given a crosstrack error  $e_{ct} = 1m$  and no orientation error

Given the complex formulation of the control law, the ordinary differential equation describing the crosstrack error over time has no analytical solution. For this reason, the convergence and stability was studied through phase plane analysis.

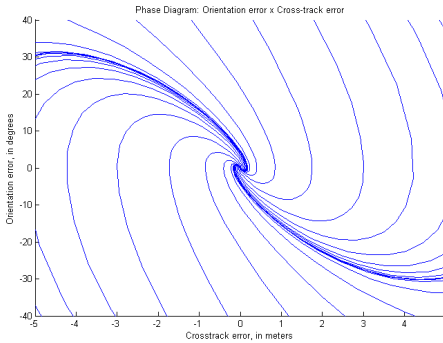


Fig. 5. Phase plane diagram

Figure 5 presents the phase plane diagram of orientation error given crosstrack error at vehicle speed  $v = 10m/s$  using a vehicle model with actuation delay and tire slip. From the diagram it is observable that from any given state the dynamic system converges to the attractor located at the origin with the error norm decreasing asymptotically even though each error measure does not.

#### IV. EXPERIMENTAL RESULTS

This section describes four experiments to demonstrate the performance of the control laws. The first experiment shows the speed tracking capability of the longitudinal controller. The second experiment used MORSE simulator [13] and the third and fourth experiments show two tracks executed inside University of São Paulo campus.

The CaRINA 2 vehicle used for the experimental tests is a Fiat Palio Adventure 2011 modified for computational control of steering, throttle, and brake. It is loaded with

several sensors such as a camera and a 3D LIDAR. Speed information is provided by the vehicle's onboard CAN bus at approximately 5Hz. Vehicle localization is provided by a Septentrio GPS System with RTK correction and IMU integration operating at 10Hz. Two onboard computers running Ubuntu Linux and ROS (Robot Operating System) are used to process information.

##### A. Longitudinal control experiment

For the longitudinal control experiment a path consisting of 4.4 kilometers of one-way two lane roads was used. This path took 6 minutes and 27 seconds to be traveled at an average speed of  $40.86Km/h$ . Figures 6 and 7 show two significative parts of this track with the reference speed in blue and the vehicle speed in red. In this experiment acceleration was limited to 20% of throttle pedal course and braking pedal was limited at 80% for non-emergency situations and unbounded for emergency situations.

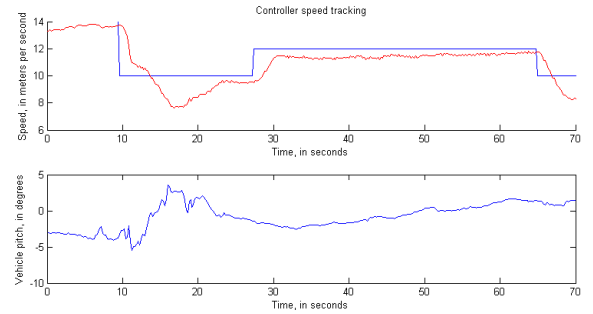


Fig. 6. Speed and pitch profile

Figure 6 presents a worst case speed tracking starting at time  $t = 10s$  where the controller reference is set from  $14m/s$  to  $10m/s$  when the car is on ascent. Causing the vehicle speed to go as low as  $7m/s$  in result of actuation delays on the brake pedal. It also presents its capability to recover from such a error and posterior convergence in less than 10 seconds.

The ability to maintain a speed when the road inclination changes is depicted in Figure 7, in highlight the cases between time  $t = 10s$  and  $t = 20s$  and for  $t > 70s$ . These cases show how the controller is capable of following and keeping, respectively, the reference speed on a highly irregular road. It also shows a non-emergency stop at  $t = 22s$ .

Since the reference speed is given by maximum allowed speed in the road or turn, the controller was designed to avoid overshoots even in detrimental of its performance. Presented results show that the vehicle speed is almost at all times lower than the reference speed to avoid exceeding those limits.

##### B. MORSE Simulation

In order to experiment with different controller setups and environments, the vehicle was modeled in Blender and used in the MORSE simulator, this model accounted for steering



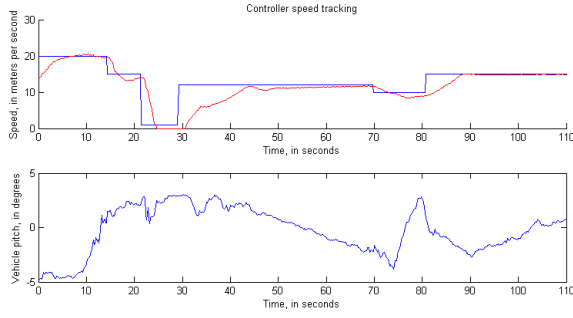


Fig. 7. Speed and pitch profile

encoder errors, IMU orientation errors, localization errors and steering speed limitation, to obtain results as close to real as possible.

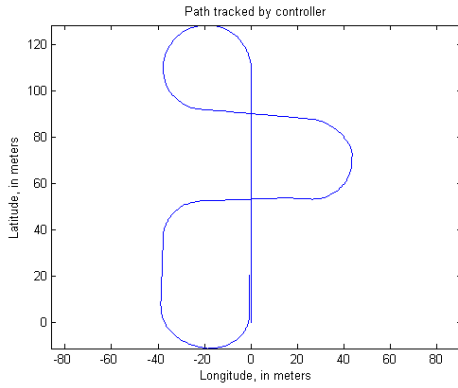


Fig. 8. Path performed in MORSE simulator

The simulator was used during the design and prototyping of the lateral control law, since it does not model longitudinal forces applied in the vehicle. The simulated track, shown in Figure 8 was 400 meters long with closed and open turn enabling the reproduction of several different vehicle behaviors. The virtual vehicle traveled at an average speed  $31.3\text{Km/h}$  and a maximum speed of  $90\text{Km/h}$ . During 5 simulation laps the mean crosstrack error was approximately zero with a standard deviation of  $0.0808\text{m}$  and the average orientation error was  $0.6327$  degrees with a standard deviation of  $2.0173$  degrees, as shown in the histogram presented at Figure 9.

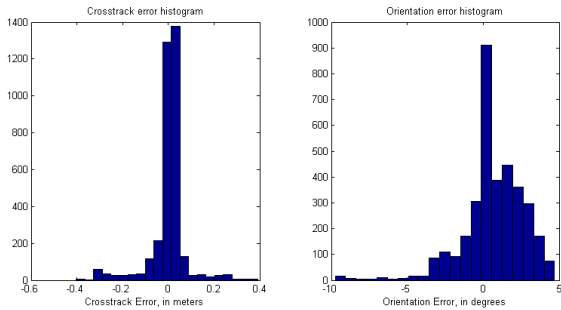


Fig. 9. Crosstrack and Orientation error histogram of the simulation

### C. Campus track 1

The first test for the lateral controller took place in a 600 meter long loop track. The trajectory consisted of one-way asphalt roads with two lanes at all times, had a high curvature left turn and a roundabout as shown in figure 10. It descends in direction of the roundabout and ascends in direction of the U-turn.

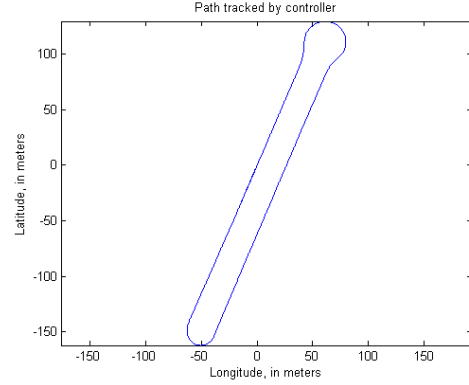


Fig. 10. Trial path inside university campus

This path was chosen for its short length and different curvatures, enabling a fast prototyping and performance evaluation. Therefore this track was used for the first controller tests and evaluation of possible values for parameter  $h$  and  $d_0$ . For performance measure in this track, the car traveled 3 laps around it with an average speed of  $20.4\text{Km/h}$  and a maximum speed of  $28.8\text{Km/h}$ . In these laps the controller presented approximately zero mean crosstrack error with standard deviation of  $0.0971\text{m}$  and a mean orientation error of  $-1.0397$  degrees with standard deviation of  $1.0397$  degrees. A histogram of crosstrack and orientation error is shown in Figure 11.

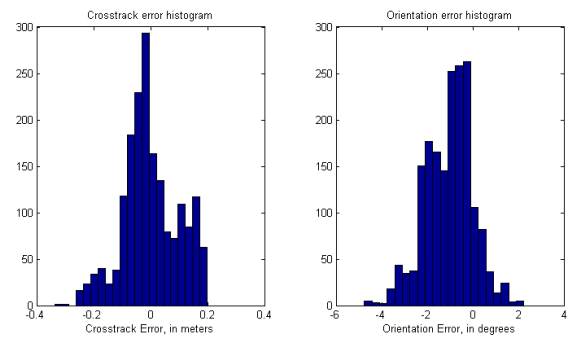


Fig. 11. Crosstrack and Orientation error histogram of the first track

### D. Campus track 2

The second test track was a 1.6 kilometers long loop going through 4 roundabouts, with single lane two-ways and two lanes one-way asphalt roads shown in Figure 12. It also had many climbs and descends along the path. This experiment provides many significative cases, like long straight roads,

high and low curvature left and right turns, useful to evaluate the performance of the control law.

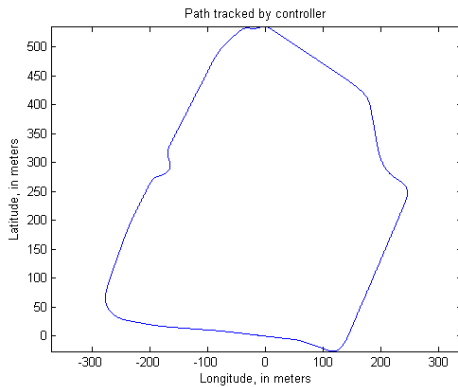


Fig. 12. Validation path inside university campus

As in the previous track, the vehicle traveled 3 laps around the path with an average speed of  $23.9\text{ km/h}$  obtaining an approximately zero mean crosstrack error with  $0.088\text{ m}$  standard deviation and a mean orientation error of  $0.9225$  degrees with a standard deviation of  $1.0544$  degrees.

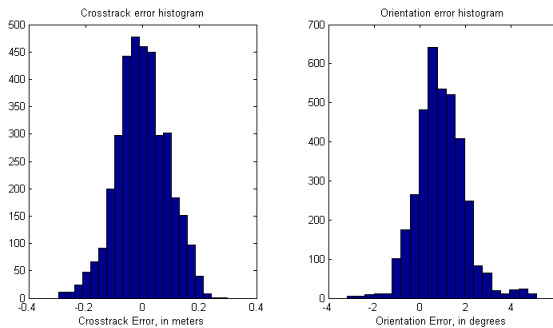


Fig. 13. Crosstrack and Orientation error histogram of the second track

Highest crosstrack and orientation errors occurred during the roundabout entrance and exit because of the curvature inversion and in high curvature turn entrances. The higher crosstrack errors in these regions appear because of the actuation maximum speed and delays in the steering and braking, limiting the possible trackable curvature rate of change. The controller kept the crosstrack error below  $0.1\text{ m}$  in straight roads although it had a small, low frequency oscillatory effect (predicted on the phase diagram in Figure 5).

In both tracks the maximum speed was limited because the tests were performed in streets inside the university campus. A previous version of the controller has also been evaluated in the city streets at  $40\text{ km/h}$  with very satisfactory results<sup>1</sup>.

## V. CONCLUSIONS

This paper describes the control laws used in CARINA project, a traditional longitudinal proportional controller

which takes the rate of change in the reference speed, and a novel lateral controller based on Bézier curves where it's possible to define how the vehicle will approach the objective path. Such controller depends on only on parameter,  $\sigma$ , which can be defined through minimization.

Future work includes take into consideration the air drag and internal resistances in the longitudinal vehicle model and the tire slip in lateral control laws. It is also planned the addition of a crosstrack error and yaw rate feedback term for the curve approach in order to reduce oscillations and improve convergence and the comparison to other tracking control laws.

## REFERENCES

- [1] J. M. Snider, "Automatic steering methods for autonomous automobile path tracking," Robotics Institute, Carnegie Mellon University, Tech. Rep. CMU-RI-TR-09-08, 2009.
- [2] O. Amidi, "Integrated mobile robot control," Robotics Institute, Pittsburgh, PA, Tech. Rep. CMU-RI-TR-90-17, May 1990.
- [3] A. Ollero and G. Heredia, "Stability analysis of mobile robot path tracking," in *Intelligent Robots and Systems 95. 'Human Robot Interaction and Cooperative Robots', Proceedings. 1995 IEEE/RSJ International Conference on*, vol. 3, 1995, pp. 461–466 vol.3.
- [4] C. Urmson, C. Ragusa, D. Ray, J. Anhalt, D. Bartz, T. Galatali, A. Gutierrez, J. Johnston, S. Harbaugh, H. "Yu" Kato, W. Messner, N. Miller, K. Peterson, B. Smith, J. Snider, S. Spiker, J. Ziegler, W. "Red" Whittaker, M. Clark, P. Koon, A. Mosher, and J. Struble, "A robust approach to high-speed navigation for unrehearsed desert terrain," *Journal of Field Robotics*, vol. 23, no. 8, pp. 467–508, 2006. [Online]. Available: <http://dx.doi.org/10.1002/rob.20126>
- [5] G. Hoffmann, C. Tomlin, D. Montemerlo, and S. Thrun, "Autonomous automobile trajectory tracking for off-road driving: Controller design, experimental validation and racing," in *American Control Conference, 2007. ACC '07*, 2007, pp. 2296–2301.
- [6] C. Urmson, J. Anhalt, H. Bae, J. A. D. Bagnell, C. R. Baker, R. E. Bittner, T. Brown, M. N. Clark, M. Darms, D. Demitrish, J. M. Dolan, D. Duggins, D. Ferguson, T. Galatali, C. M. Geyer, M. Gittleman, S. Harbaugh, M. Hebert, T. Howard, S. Kolski, M. Likhachev, B. Litkoushi, A. Kelly, M. McNaughton, N. Miller, J. Nickolaou, K. Peterson, B. Pilnick, R. Rajkumar, P. Rybski, V. Sadkar, B. Salesky, Y.-W. Seo, S. Singh, J. M. Snider, J. C. Struble, A. T. Stentz, M. Taylor, W. R. L. Whittaker, Z. Wolkowicki, W. Zhang, and J. Ziegler, "Autonomous driving in urban environments: Boss and the urban challenge," *Journal of Field Robotics Special Issue on the 2007 DARPA Urban Challenge, Part I*, vol. 25, no. 8, pp. 425–466, June 2008.
- [7] U. Ozguner, T. Acarman, and K. Redmill, *Autonomous Ground Vehicles*, ser. Artech House ITS series. Artech House, 2011. [Online]. Available: <http://books.google.com.br/books?id=LkjoHNGoJF4C>
- [8] K. Osman, M. Rahmat, and M. Ahmad, "Modelling and controller design for a cruise control system," in *Signal Processing Its Applications, 2009. CSPA 2009. 5th International Colloquium on*, 2009, pp. 254–258.
- [9] P. Falcone, F. Borrelli, J. Asgari, H. Tseng, and D. Hrovat, "Predictive active steering control for autonomous vehicle systems," *Control Systems Technology, IEEE Transactions on*, vol. 15, no. 3, pp. 566–580, 2007.
- [10] Z. Qu, *Cooperative control of dynamical systems: applications to autonomous vehicles*. Springer, 2009.
- [11] J.-w. Choi, R. Curry, and G. Elkaim, "Path planning based on bezier curve for autonomous ground vehicles," in *World Congress on Engineering and Computer Science 2008, WCECS'08. Advances in Electrical and Electronics Engineering-IAENG Special Edition of the*. IEEE, 2008, pp. 158–166.
- [12] K. Jolly, R. Sreerama Kumar, and R. Vijayakumar, "A bezier curve based path planning in a multi-agent robot soccer system without violating the acceleration limits," *Robotics and Autonomous Systems*, vol. 57, no. 1, pp. 23–33, 2009.
- [13] G. Echeverria, N. Lassabe, A. Degroote, and S. Lemaignan, "Modular open robots simulation engine: Morse," in *Robotics and Automation (ICRA), 2011 IEEE International Conference on*. IEEE, 2011, pp. 46–51.

<sup>1</sup><https://www.youtube.com/watch?v=IyPNdN8Hu8>